



Evaluation of eco-friendly cellulose and lignocellulose nanofibers from rice straw using Multiple Quality Index

Mohamed Taha^{a,b,c} Mohammad L. Hassan^{d*}, Montasser Dewidare^{e,f}, M.A. kamel^g, W. Y. Ali^g,



CrossMark

Alain Dufresne^e

^aMechanical Engineering Department, College of Engineering and Technology, Arab Academy of Science, Technology and Maritime Transport, Sadat Road - P.O. Box 11, Aswan, Egypt.

^bDepartment of Materials Engineering and Mechanical Design, Faculty of Energy Engineering, Aswan University, Aswan, 81542, Egypt.

^cUniv. Grenoble Alpes, CNRS, Grenoble INP, LGP2, F-38000 Grenoble, France.

^dCellulose and Paper Department and Centre of Excellence for Advanced Sciences, National Research Centre, 33 El - Buhouth street, Dokki 12622, Giza, Egypt

^eDepartment of Mechanical Engineering, Faculty of Engineering, Kafr Elsheikh University, El-gaish Street, Kafr El Sheikh, Egypt.

^fHigher Institute of Engineering and Technology, Kafrelsheikh 33516, Egypt.

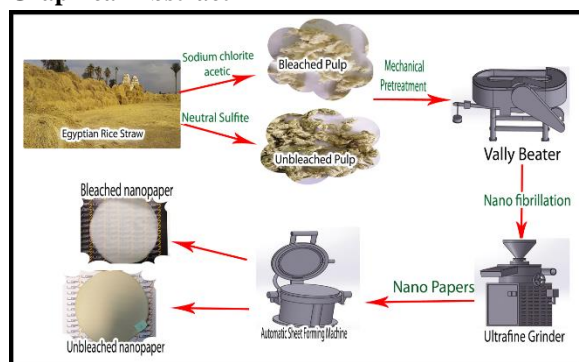
^gFaculty of Engineering, Minia University, Minia, Egypt.

Abstract

Huge amounts of rice straw are left every year in different areas of the world; these residues still cause environmental problems due to un-safe practices such as burning. Isolation of nanomaterials such as cellulose nanofibers represents an effective way for utilization of rice straw in advanced products. The current work aimed at evaluating the properties of rice straw cellulose nanofibers isolated from bleached and high-lignin unbleached pulps using a multi-criterion quality index, which allows a benchmarking analysis between different sources, processes and features. Rice straw was subjected to neutral sulfite pulping process to obtain the high-lignin unbleached pulp while the bleached pulp was obtained by bleaching the produced pulp with NaClO₂/acetic acid mixture. Using mechanical pretreatment (Valley beater), and ultrafine friction grinder both bleached and unbleached pulps were used to obtain cellulose nanofibers with and without lignin (LRSNF and RSNF, respectively). Nanopaper sheets were prepared from both types of nanofibers and characterized using tensile tests, optical microscopy, atomic force microscopy, electron scanning microscopy, water contact angle and surface energy. Cellulose nanofibers generated from rice straw were scored using a multi-criterion quality index depending on characterization using eight tests (nanosized and macro size fraction, turbidity, Young's modulus, porosity, transmittance, tear resistance, and homogeneity).

Keywords: Rice straw; Rice Straw nanofibers (RSNF); Lignocellulose Rice Straw nanofibers (LRSNF); Nanopaper properties; Quality Index.

Graphical Abstract



1. Introduction

Intensive research has been carried out during last decades on the isolation of cellulose nanofibers from various lignocellulosic materials. Most of these studies investigated isolating cellulose nanofibrils from lignin-free (bleached) pulp. Besides their high yield, cost savings and reduced emissions from bleaching cycles, unbleached fibers comprising residual lignin, hemicelluloses and extractives provide an alternative raw material for the production of lignocellulose nanofibrils (LRSNF). In addition, the presence of lignin at the surface and within the nanofibers is another feature that can affect properties of the

*Corresponding author e-mail: mlhassan2012@yahoo.com (Mohammad Hassan).

Receive Date: 26 May 2021, Revise Date: 19 June 2021, Accept Date: 21 June 2021

DOI: 10.21608/ejchem.2021.77618.3800

©2021 National Information and Documentation Center (NIDOC)

nanofibers and nanocomposites (1, 2). For many years, rice cultivation has been a strategic crop all over the world as it contributes to the global economy. It produces vast quantities of straw, which is a burden that farmers consider difficult to get rid of easily. Practice of rice straw burning is unfortunately very common in some areas. It has deep environmental impact. One of the interesting ways of using this useful bioresource is cellulose extraction. Cellulose is a desirable polymer because of its abundance, renewability and fascinating mechanical properties, providing possible solutions to the growing demand for environmentally sustainable materials as an alternative to materials made from petroleum. Rice straw is also gaining growing importance as a raw material for fuel, chemical, paper, building and food packaging industries (3-5).

Rice straw, contains high silica content of 9–14 % which, rendering its alkaline pulping undesirable due to silica dissolving in the pulping liquor (black liquor). Therefore, the black liquor concentration for the recovery of excess alkali or energy output is a challenge as the liquor needs more treatments before use. Nonetheless, rice straw alkali pulp has typically a low lignin content and can be easily bleached to produce pulp for various types of paper. Neutral pulping methods are effective solutions for avoiding difficulties raised from alkaline rice straw pulping. Neutral sulfite pulping is a proper method for obtaining high-yield pulp (~90%) with high lignin content. The sulfite pulping induces a minor modification of the lignin structure without substantial removal of lignin, and in addition, the pulp obtained is generally suitable for producing paperboards (2, 6, 7).

For each raw material, different properties of RSNFs could be obtained due to the numerous possible combinations of pretreatments and method of fibrillation(8-10). Therefore, criteria and methods need to be established to create an objective quality-related value for the RSNF in order to optimize the production processes and choose the appropriate final application. The quality of RSNF produced could be calculated with numerous parameters. The Technical Association of the Pulp and Paper Industry (TAPPI) has suggested common terminology for the classification of nano cellulose materials (TAPPI WI 3021) based on the size and aspect ratio. Significant progress has been made on characterization methods over the past decade. Previous state-of-the-art research (11) put forward tens of analytical methods focused on quality of nanomaterials, namely distribution of particle size, rheology, mechanical properties, crystallinity, morphology, and surface chemical. Although the combination of such methods may result in an accurate representation of the suspension, such a list of analyses usually needs some costly,

complicated, and time-consuming tools. They also require expertise and do not enable comparisons.

Consequently, it becomes important to have more easily accessible and efficient methods of comparison to monitor the quality of the various available grades. Such approaches would also permit the reproducibility of the conformity and quality assurance manufacturing procedure. The literature showed some studies relied only on size of the nanofibrils (so-called degree of fibrillation) as a single criterion analysis, neglecting the suspension's higher-scale (12). Other studies focused on multi criteria approaches to nanofibers suspension comparisons (13, 14). Nevertheless, they have not yet offered a simple or standard method of comparison. The so-called "fibrillation yield" has been also used as a measure for fibrillation depending on centrifugation technique (13, 15-19). The ability of CNFs to transmit or diffuse visible light can also be correlated with the degree of fibrillation (20), in both nanofibers suspensions (17, 21) and films(14). Light scattering, light transmittance, and turbidity measurement by UV-visible spectroscopy have been also used to assess the quality of CNFs (13, 22). The disadvantage of using purely optical methods is the accuracy because only small areas containing nanofibrils are characterized, except "microfibers" that are poorly fibrillated. Other high-level microscopy methods are difficult to implement in a production plant to evaluate the quality of CNFs. In particular, a publication by Chinga-Carrasco (23) based on the comparison of optical methods for evaluating the degree of CNFs fibrillation using an image scanner enables the characterization of nanoparticles as well as residual fibers. Such a system seems promising for evaluating CNFS online quality processes. Another approach for measuring the quality of CNFs was focused on mechanical fractionation (24) and degree of polymerization of CNFs (25). Recently, a multi-criteria approach has been proposed by Desmaisons et al. (26) that would produce a single quantitative parameter (quality index) enabling industrial and laboratory monitoring of the output of CNFs. The proposed quality index takes the data of several testing results and put them into an equation to get a metric measure (out of 10) as a quality of the CNFs.

The developed environmentally friendly materials have numerous intriguing applications, as waste water treatment(27, 28), tribology applications(29), 3 D printing(30, 31) and biomedical applications(32, 33). The current work studied application of a Multifactorial "quality Index" (QI) for evaluating the quality of rice straw nanofibers (RSNF) isolated from bleached and unbleached rice straw pulps based on results of eight tests (physical, optical, and mechanical testing) on RSNF suspension and nanopaper sheets.

2- Materials and methods.

2.1 Materials

Rice straw was obtained from local farms in Giza, Egypt. To remove the dust, the straw was washed with tap water H₂O, and left to air dry. Sodium carbonate, sodium sulfite, sodium chlorite (technical grade 80%), and glacial acetic acid were chemicals of reagent grade and used as Fisher Scientific (Loughborough, UK) obtained.

2.2 Preparation of neutral sulfite rice straw pulp

Unbleached neutral sulfite rice straw pulp was prepared by pulping the rice straw in aqueous solution containing 10% sodium sulfite (based on rice straw weight) and 2% sodium carbonate, at 160°C for 2 h, as described earlier in Hassan et al (2). The chemical composition of the pulp was analyzed using standard methods to determine the ash content, Klason lignin, insoluble acid lignin, α -cellulose, and pentosans (34). The produced pulp was bleached using a sodium chlorite/acetic acid mixture at 80 °C according to the previously published method (35).

2.3 Mechanical pretreatment

The bleached and unbleached pulps suspensions were refined with a disk refiner (Valley Beater) at 2 wt. % in water to a drainage level of 90 °SR (ISO 5267-1). Measures were tripled, at least.

2.4 Isolation of rice straw nanofibers

RSNF from bleached and LRSNF from unbleached rice straw pulp were extracted according to our protocol model. A suspension containing 2 wt.% RSNF was fibrillated using a Super masscolloider ultra-fine friction grinder (Model MKZA6-2, disk model MKG-C 80, Masuko Sangyo Co., Ltd., Kawaguchi, Japan) equipped with recirculation. The protocol model designed as one loop is equivalent to 10 paths in the same distance gap between 0,-5 and -10 μ m disks and 1500 rpm movement speeds.

2.5 Nanopaper preparation

Nanopapers from bleached and unbleached RSNF were prepared using a former hand sheet (Rapid Kothen, ISO 5269-2) and 2 g RSNF (dry content) diluted in deionized water to 0.5%. The suspension was filtered under vacuum at 800 mbar on a 1 μ m nylon sieve until the supernatant water was removed. The layer was then vacuum-dried at 85 °C for 20 minutes between two 1 μ m nylon sieves sandwiched between two rectangular oval cartons. The nanopapers were kept in a conditioned room for 48 h at 23° C and 50% RH prior to characterization.

2.6 Optical microscopy

The complete fibrillation of bleached and unbleached RSNF suspensions was checked using optical

microscopy (Carl Zeiss Axio Imager M1 fitted with a digital camera AxioCam MRc 5) by disappearing of the micro-size fibers during the ultra-fine grinding. For each sample at least five pictures have been taken and the most appropriate ones are shown.

2.7 Scanning electron microscopy – Energy dispersive spectrum (SEM-EDS)

The morphology of the prepared RSNF was conducted by scanning electron microscopy (SEM) using ESEM (Quanta 200, FEI, Japan) fitted with EDS unit, including dispersive energy spectrum. At least 5 sample pictures were taken, and the most appropriate picture was chosen.

2.8 Atomic force microscopy (AFM)

The RSNF dimensions were defined by AFM (Nanoscope III[®], Bruker). The RSNF sample was diluted up to 1×10^{-6} wt %, and spread with a high-shear homogenizer (Ultraturrax[®], IKA). Then, a drop of this distilled solution was placed on a mica substrate and dried at room temperature overnight. AFM images were acquired with a silicon cantilever (OTESPA[®], möglich, IKA) in the tapping mode at various places. At least 5 photographs have been sampled from 5 different locations and the most representative is presented here.

2.9 XRD

The X-ray diffraction (XRD) patterns of RSNF were recorded using an Empyrean X-ray diffractometer (PANalytical, The Netherlands). The crystallinity index was calculated from the XRD patterns according to the following equation (36): $CrI = (I_{002} - I_{am})/I_{002}$, where I_{002} is the intensity of the diffraction profile at the position of the 002 peak ($2\theta = 22.7^\circ$) and I_{am} is the intensity at approximately $2\theta = 18^\circ$.(37)

2.10 TGA

The thermal stability of RSNF was examined with TGA using Perkin Elmer thermogravimetric analyzer. The heating rate was set at 10°C/min over a temperature range of 50–800 °C. Measurements were carried out in a nitrogen atmosphere at a flow rate of 50 cm³/min.

2.11 Contact angle and surface energy measurements

Measurements of the contact angle and surface energy were performed using the fully automated Data Physics optical contact angle microliter dosing method (OCA 40 Micro) based on images. Liquid drops (2 μ l / drop) of DI water (more polar), ethylene glycol, ethylene glycol in H₂O 60% (intermediate polar & dispersive), and diiodomethane (mostly dispersive) with established surface tensions were used. The contact angle for each dispensed liquid droplet was

calculated at 22 ° C and 45 %RH conditions and a video was captured (72 frames / second). Using this approach any subtle changes to the droplet on the surface can be observed precisely. This method makes the calculation of 0.1 ° precision touch angles. The contact angle for the four different tested fluids and the surface free energy (polar and dispersive components) were evaluated from the sessile drop technique and Owens, Wendt, Rabel and Kaelble (OWRK) model, respectively.

2.12 Mechanical properties

The mechanical properties of the nanopapers (tensile strength, elongation at break, and Young's modulus) were determined using an Instron 5965 system equipped with a 5 kN capacity load cell in accordance with the ASTM D638 standard. Specimens of 65 mm × 15 mm with an average thickness of 60 μm were prepared for each sample and conditioned at 25 °C for 48 h and 50 % RH before testing with a crosshead speed of 2 mm s⁻¹.

2.13 Tear resistance

The tear resistance was measured using a tear tester from Noviprofibre (Elmendorf, France) fitted with a 4000 mN pendulum. The instrument tests the force required to tear a sample out of the plane, and two types of measurements have been performed; tear resistance after initiation by cutting a primer and tear resistance without using any primer. When the crack is formed, the former gives the force required to sustain a break, while the latter gives the strength needed to start the crack. The test specimen dimensions were 65 × 50 mm² and for each RSNF four samples were tested.

2.14 Light transmittance

With an ultraviolet-visible spectrometer (UV 1800, Shimadzu, Japan), the light transmission through RSNF nanopapers was measured at 550 nm. Five tests on samples from at least three separate nanopapers were performed for each sample. Total number of repeats was 15.

2.15 Nanosized fraction

The study of the nanosized fractions was carried out according to the protocol defined by Naderi et al. [19]. RSNF suspensions were diluted to 0.02 wt% and centrifuged at 1000 g for 15 min with a Sigma 3–18 KS Germany centrifuge. Tests had been at least six.

2.16 Turbidity

A portable turbidimeter (AL 250T-IT) with a technique range of 0.01–1100 NTU was used to

calculate the turbidity of a 0.1 % wt. RSNF suspension. Ten measurements were performed for each suspension and used to get a mean value.

2.17 Average size of the microparticles

RSNF suspension microscopic images were described with the software Image J (26). After the images were converted to 8-byte form and thresholding, the average size of the remaining particles was obtained using the "particle analysis" function. The data corresponded to the total surface area divided by the number of particles counted. This test characterizes the residual fibers that were not fibrillated.

2.18 Quality index

LRSNF and RSNF were evaluated according to the Quality Index (QI) created by Desmaisons et al. (26). The quality index is defined as the weighted sum of the marks to convert each isolated equation linearly into one single equation with eight coefficients.

QI = 2 * Nanosized fraction mark + 2 * Turbidity mark + 1 * Young's Modulus mark + 1 * Porosity mark + 1 * Transmittance mark + 1 * Tear resistance mark + 1 * Macro size mark + 1 * Homogeneity mark (1)

$$Q.I. = 0.20 x_1 + (-0.02 x_2) - 0.035 x_3^2 + 1.27 x_3 - 0.16 x_4 + 1.65 \ln(x_5) - 3.59 \ln(x_6) - 2.67 \ln(x_7) + 0.18 x_8 + 69.6 \quad (2)$$

With x_1 the nano fraction (%), x_2 the turbidity (NTU), x_3 the Young's modulus (GPa), x_4 the porosity (%), x_5 the tear resistance (mN), x_7 the macroscopic homogeneity (%) and x_8 the macroscopic homogeneity.

3. Results and discussion

The RSNF from bleached rice straw pulp and the LRSNF from unbleached rice straw pulp were investigated.

3.1 Morphology of the prepared nanofibers

The chemical composition of bleached and unbleached pulps is shown in Table 1. As can be noticed from the results, the two pulps contain a high amount of silica. The bleached rice straw pulp exhibits a higher α-cellulose content with traces of lignin. The degree of polymerization (DP) of the pulps are in accordance with known values for cellulose pulp isolated from agricultural residues and also indicates that there was no significant degradation of cellulose during the pulping and bleaching process.

Table 1. Chemical composition of bleached and unbleached neutral sulfite rice straw pulp.

	α -cellulose %	Hemicellulose %	Klason lignin %	Ash content %	DP
Unbleached RS	54.12	14.34	14.15	16.63	903
Bleached RS	68.4	18.6	1.32	12.47	834

The progress of fibrillation of pulp fibers into nanofibers for both bleached and unbleached pulps was tracked by optical microscopy images as shown in Figure 1. Upon passing the pulp through grinder plates, the viscosity also increased, and when complete fibrillation was achieved, a viscosity plateau was reached. This implies the formation of a stronger network by encouraging fibril-to-fibril bonding, resulting in higher fibrillation according to Berglund et al. (38). Hassan et al. (39) studied the absence of micro-sized fibers with the producing gel-like structure as an indication of progression in fibrillation, by using optical microscopy. In that work, disappearance of the micro-fibers depended on the number of passes. In the current work, the pulp was circulated through the ultrafine grinder using a pump; one complete loop of circulation was equivalent to 10 passes through the discs. Figure 1A shows unbleached rice straw pulp before grinding, and Figures 1B-D show the images after 1 loop at zero distance between the discs, another loop at distance $-5 \mu\text{m}$, and a last loop at distance $-10 \mu\text{m}$ for RSNF, respectively, for the

unbleached pulp (LRSNF). Fig 1E shows bleached rice straw pulp before grinding, and Figures 1F-H show the images after 1 loop at zero distance between the discs, another loop at distance $-5 \mu\text{m}$, and a last loop at distance $-10 \mu\text{m}$ for RSNF for the bleached pulp (RSNF), respectively. Optical microscope images for both unbleached and bleached rice straw pulp (Figures 1A and 1E) shows how the fibrillation of the fibers' suspension rises, producing more fines and fibrillations. It could be inferred from the images for bleached rice straw pulp that degradation took place first along the fibers before fibrillation could be initiated. With the unbleached pulp, fibrillation starts during the early stages without major fiber degradation. This could affect the properties of the nanopaper made from isolated nanofibers as shown below. The images also show that after the final grinding loop, no non-fibrillated fibers could be seen in the case of unbleached rice straw while those isolated from bleached showed few non-fibrillated fibers.

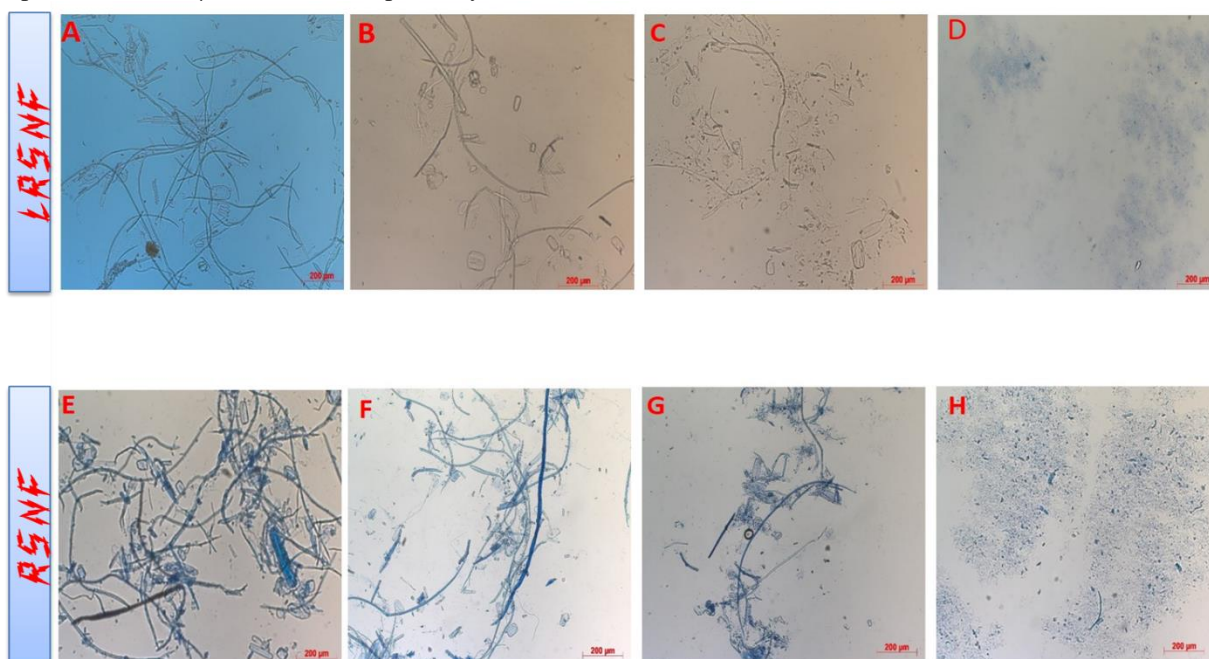


Figure 1. Optical microscopy images at scale $200\mu\text{m}$ for A) unbleached rice straw pulp before fibrillation and B, C, D unbleached rice straw pulp during grinding process depending on loops and distance. (E) bleached rice straw pulp before fibrillation and F, G, H bleached rice straw pulp during grinding process depending on loops and distance.

The morphology of RSNF prepared from unbleached and bleached was studied using scanning electron microscopy and atomic force microscopy (Figure 2).

The SEM images for LRSNF and RSNF reveal however no significant differences in the RSNF structure for bleached and unbleached pulp with the

appearance of silica particles on the surface of the fibers. The presence of silica was proved from the EDS analysis as seen in Figure 2. The LRSNF and RSNF measurements have been further clarified by AFM of extremely diluted air-dried suspensions (0.001 wt%) accumulated on freshly glued surfaces of mica (Figure

2). The AFM images for both types of pulp indicated the presence of nanofibers and nanofiber bundles (Figure 2), and also showed the presence of nano-sized spherical entities which could be silica originally presents in the pulp (40).

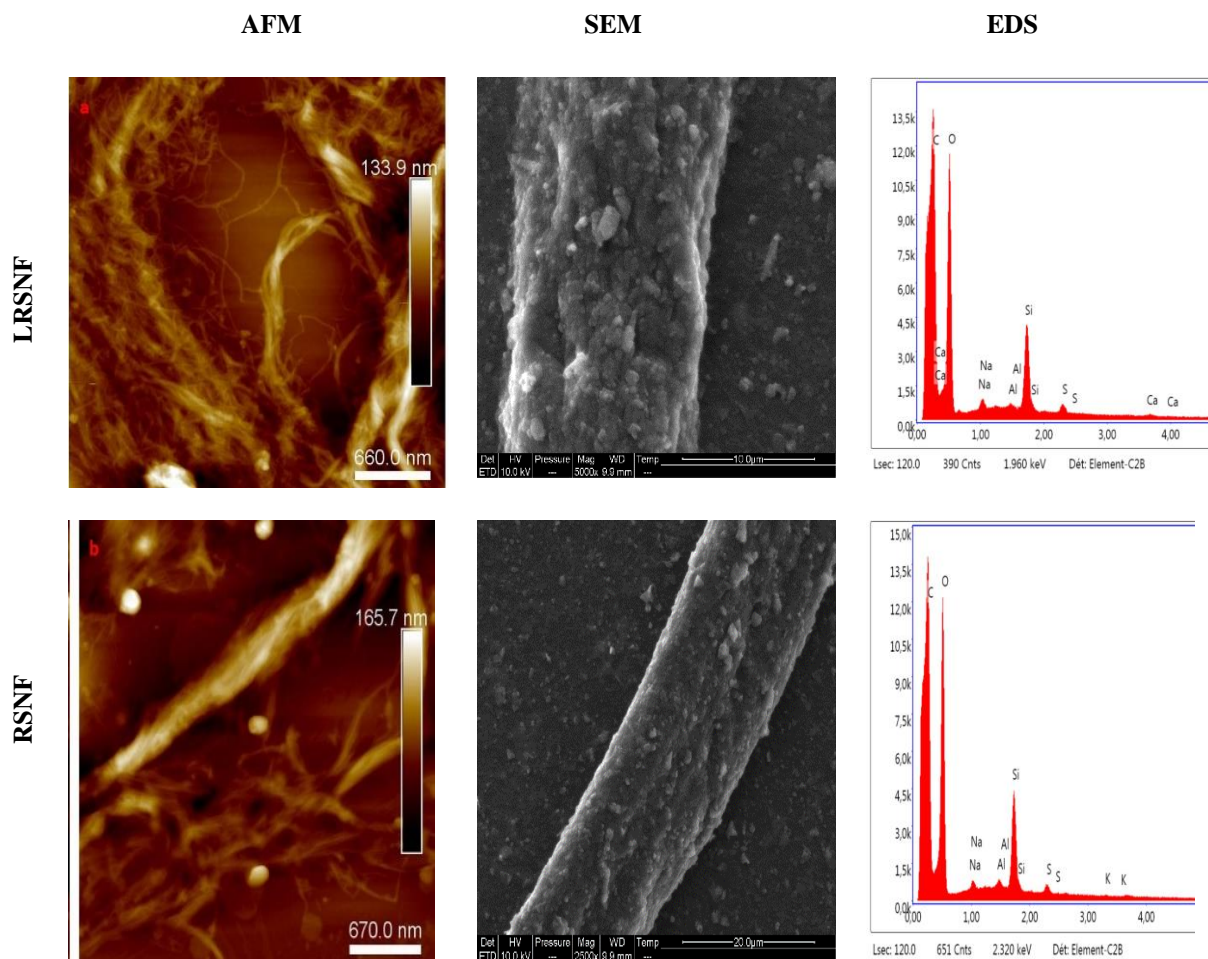


Figure 2. AFM, SEM and EDS analysis for LRSNF and RSNF.

3.2 Hydrophilicity of RSNF and LRSNF nano paper

The most significant metric for cellulosic surfaces was the contact angles and surface energy to assess their suitability for various applications. Four sampling liquids: water, ethylene glycol in H₂O 60%,

diiodomethane and ethylene glycol were selected for contact angle and surface energy studies due to their low vapor pressure and different polar and dispersive components of their surface energy. The surface energy components are shown in Table 2. The Owens-Wendt method was used to quantify the surface free energy (41).

Table 2. Surface tension (SFT) of the test liquids

Liquid	SFT (Total) [mN/m] γ_1	SFT(Dispersive) [mN/m] γ^d	SFT (Polar) [mN/m] γ^p	Values Adapted From
Water	72.3	18.7	53.6	Rabel et.al. (42)
Ethylene glycol in H₂O 60%	55.86	19.79	36.07	Janczuk et al. (43)
Diiodomethane	50.8	49.5	1.3	Owens et al. (41)
Ethylene glycol	47.7	26.4	21.3	Gebhardt et al. (44)

For the LRSNF and RSNF nanopapers, the mean contact angle (CA) value for the four tested fluids was measured in the surface energy assessment, as summarized in Table 3. The contact angle values for LRSNF and RSNF were very close to each other for the different liquids except in the case of water where LRSNF nanopaper had a higher contact angle than RSNF, probably due to less lignin in the former. Nevertheless, the combination of the results for the four liquids allowed more effectively to reveal the subtleties of surface energy. A solid's surface-free

energy is a characteristic parameter that significantly impacts many interfacial processes such as adherence, wetting, and absorption. Table 3 displays the values obtained for γ^d and γ^p , as well as the total surface energy γ_1 . The LRSNF nanopaper had slightly higher total surface energy (γ_1) and polar surface energy (γ^p) than that of RSNF due to the higher lignin content in the former. The LRSNF still has good hydrophilicity. Hydrophilic nature of LRSNF has been studied in a previous study (2).

Table 3 Data obtained from wetting measurements with the four liquids and calculated surface energies for LRSNF and RSNF

S/N	Sample	Water CA (°)	Ethylene glycol in H2O 60% CA (°)	Diiodomethane CA (°)	Ethylene glycol CA (°)	Surface Energy Total (mN/m)	Surface Energy Polar (mN/m)	Surface Energy Dispersive (mN/m)	Convergence
1	LRSNF	31.6±2.1	20.7 ±1	51 ±2.3	11.7±2.7	55.9	38	17.9	0.9000
2	RSNF	26.5±2.9	21.5±1	52.1±2.7	12.6±4.4	53.3	35.2	18.1	0.8569

3.3 X-ray diffraction of the prepared nanopapers

The X-ray diffraction patterns for nanopaper sheets are shown in Figure 3 and the crystallinity index was determined according to Segal method (45). As shown in Figure 3, the characteristic peaks of native cellulose associated to planes (110) and (200) around 15° and 22°, respectively, are observed for RSNF and LRSNF. The crystallinity index was found to be 65 and 71 % for LRSNF and RSNF, respectively. The slightly higher crystallinity for RSNF than for LRSNF is due to the higher α -cellulose content for the former.

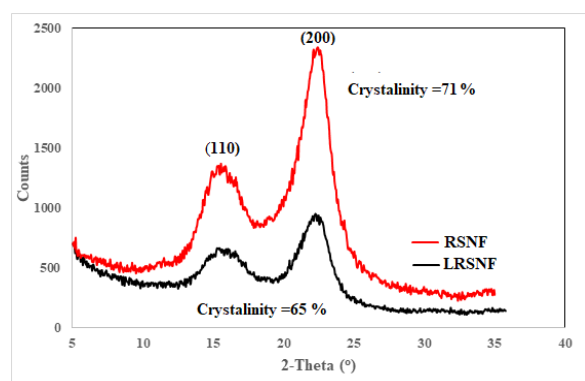


Figure 3. XRD patterns for RSNF and LRSNF

3.4 Thermogravimetric analysis (TGA) of the prepared RSNF and LRSNF

The thermal stability of both RSNF and LRSNF prepared from bleached and unbleached pulp (RSNF and LRSNF) was studied using thermogravimetric analysis. As can be seen in Figure 4, the higher thermal stability of LRSNF compared to RSNF could be due to the presence of lignin which has higher thermal stability (46). The first degradation step for RSNF and LRSNF started at 265 °C and 300 °C, respectively, as

the degradation of hemicelluloses. The second degradation step for RSNF and LRSNF occurred at 350 and 380 °C, respectively. During this stage, the weight loss could be attributed to cellulose decomposition; and degradation of lignin, the most stable component (47, 48). Finally, at temperatures higher than 500 °C, the decomposition is due to the complete oxidation of the remaining organic materials (49). The char content for RSNF and LRSNF was found to be 40 and 60 %, respectively.

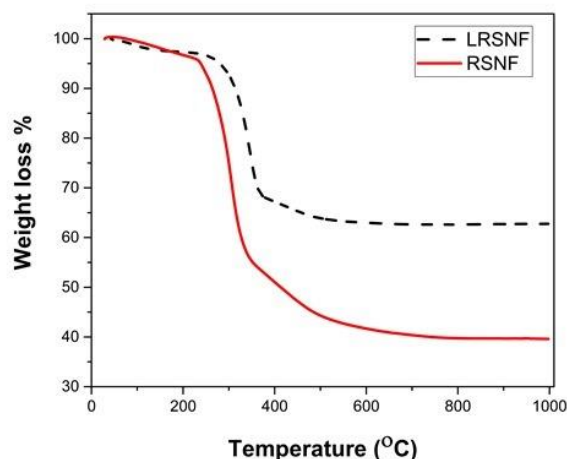


Figure 4. TGA for RSNF and LRSNF.

3.5 Mechanical properties and quality index calculation

The typical stress-strain curves for the RSNF and LRSNF nanopaper are presented in figure 5. It can be clearly seen from the figure that the tensile strength of the nanopaper prepared from RSNF with lignin (83.3 MPa) is higher than that without lignin (74.2 MPa). This result suggested that the residual lignin had the role of a cementing agent. The Young's modulus for

the RSNF and LRSNF nanopaper was found to be 6.3 and 6.7 GPa, respectively, which is in the range found in previous publications (2, 50, 51).

3.6 Quality index evaluation

The properties of the RSNF prepared from bleached and unbleached rice straw pulps were further evaluated using a multi-scale quality index. The turbidity, nanosize fraction, and light transmittance of the fiber suspensions were measured and the results are presented in Table 5. The LRSNF suspension had a lower residual microfiber content than that of RSNF indicating better fibrillation. This was confirmed by the nanosized fraction values which were 78% and 67% for LRSNF and RSNF, respectively. These values are in accordance with previous studies for CNF isolated from different lignocellulosic materials (19, 52, 53). The nanofiber aggregation for LRSNF was proved by the high turbidity (404 NTU) and porosity of the nanopaper (40.1 %) compared to RSNF. The tear resistance for the LRSNF nanopaper was lower than for RSNF.

Cellulosic nanofiber quality is important to quantify (11, 54). Desmaisons et al. proposed a multi-criteria approach to obtain the quality index of cellulose nanofiber suspensions under the framework of a unique quantitative grade (26). In that study, the quality index of RSNF from bleached pulp could be estimated. For the best of our knowledge, the

application of the multi-criteria approach to calculate quality index for RSNF isolated from unbleached pulp was rarely studied (55). According to the multi-criteria approach, the Quality Index was calculated using average area of residual microfibrils, nanosized fraction, turbidity of suspension, and Young's modulus of the nanopaper prepared from LRSNF and RSNF. As shown in Table 5, higher quality index was obtained for LRSNF than that of RSNF, indicating better quality of nanofibers isolated from the unbleached rice straw pulp (26, 52, 53, 55, 56).

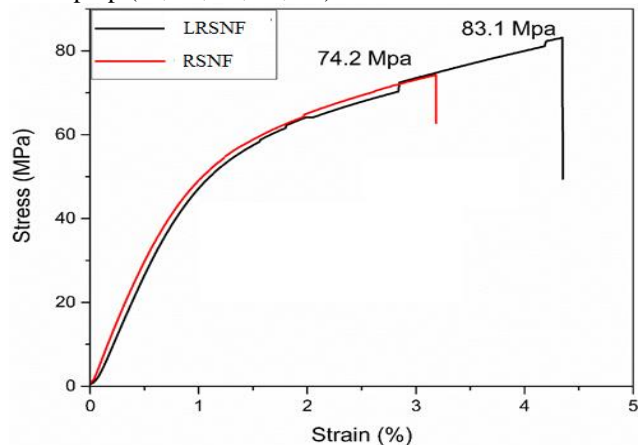


Figure 5. Stress-strain curves for LRSNF and RSNF nanopapers

Table 4 Optical and mechanical properties for LRSNF and RSNF suspension and/or nanopaper and the calculated quality index.

	Nanosized fraction (%)	Turbidity (NTU)	Transmittance (%)	Young's modulus (GPa)	Tear resistance	Porosity (%)	Quality Index
LRSNF	78.86±3.9	404±9.6	18.63	6.3±0.2	33±0.9	40.1±4.2	81±11.8
RSNF	67.57±5.5	365±9.2	27.88		37±1.2	37 ±3.1	63±3.2

Conclusion

The current work covered a comprehensive study of the variables affecting the properties of nanofibrils obtained from rice straw and a detailed characterization of the product to explain the impact of lignin on the properties of nanofibrils and nanopapers. AFM images showed very homogeneous nanosized fibers, and the presence of residual silica from rice straw pulp as nano-sized spherical individuals. The total surface energy (γ_1) and polar surface energy (γ^p) values were slightly higher in the case of LRSNF than for RSNF. Despite the presence of lignin, LRSNF had good hydrophilicity. The stress - strain curves for LRSNF and RSNF nanopapers showed higher tensile strength for nanopaper prepared from the former than

the later but LRSNF nanopaper had lower tear resistance than that made from RSNF. The eight parameters studied for the nanofibers and nanopapers prepared from RSNF and LRSNF were used to calculate the Quality Index, which was 81 and 63 for RSNF and LRSNF, respectively. The obtained Quality Index indicates good quality of nanofibers isolated from rice straw, particularly from LRSNF. Moreover, the presence of lignin had a salutary effect on the development of the cellulose nanofibers and on the final properties of the nanopapers.

Acknowledgment

The authors acknowledge funding of the current work through the grant submitted by the Institut Français

d'Égypte au Caire, Eiffel Programme scholarship and the French Ministry for Europe and Foreign Affairs. LGP2 is part of the LabEx Tec 21 (Investissements d'Avenir - grant agreement n°ANR-11-LABX-0030) and of the PolyNat Carnot Institut (Investissements d'Avenir - grant agreement n°ANR-11-CARN-030-01). Harouan Hassan from faculty of energy engineering for the computer-aided design.

Authors' contribution

The manuscript was written with contributions of all authors. All authors have given approval to the final version of the manuscript. All authors contributed equally.

Compliance with ethical standards

Conflict of interest

The authors declare that they have no conflict of interest.

Ethical approval

The authors declare the research did not involve either human participation or animal testing

References

1. E. Rojo *et al.*, Comprehensive elucidation of the effect of residual lignin on the physical, barrier, mechanical and surface properties of nanocellulose films. *Green Chemistry* **17**, 1853-1866 (2015).
2. M. Hassan, L. Berglund, E. Hassan, R. Abou-Zeid, K. Oksman, Effect of xylanase pretreatment of rice straw unbleached soda and neutral sulfite pulps on isolation of nanofibers and their properties. *Cellulose* **25**, 2939-2953 (2018).
3. M. A. S. Azizi Samir, F. Alloin, J.-Y. Sanchez, A. Dufresne, Cross-linked nanocomposite polymer electrolytes reinforced with cellulose whiskers. *Macromolecules* **37**, 4839-4844 (2004).
4. J. Desmaisons, E. Gustafsson, A. Dufresne, J. Bras, Hybrid nanopaper of cellulose nanofibrils and PET microfibers with high tear and crumpling resistance. *Cellulose* **25**, 7127-7142 (2018).
5. X. Chen, J. Yu, Z. Zhang, C. Lu, Study on structure and thermal stability properties of cellulose fibers from rice straw. *Carbohydrate polymers* **85**, 245-250 (2011).
6. J. P. Casey, Pulp and paper. Chemistry and chemical technology. (1960).
7. F. Abdel-Mohdy, E. Abdel-Halim, Y. Abu-Ayana, S. El-Sawy, Rice straw as a new resource for some beneficial uses. *Carbohydrate Polymers* **75**, 44-51 (2009).
8. J. Huang, A. Dufresne, N. Lin, *Nanocellulose: From fundamentals to advanced materials*. (John Wiley & Sons, 2019).
9. A. J. P. Dufresne, Biomaterials, Preparation and Properties of Cellulose Nanomaterials. **5**, 1-13 (2020).
10. G. Siqueira, S. Tapin-Lingua, J. Bras, D. da Silva Perez, A. Dufresne, Morphological investigation of nanoparticles obtained from combined mechanical shearing, and enzymatic and acid hydrolysis of sisal fibers. *Cellulose* **17**, 1147-1158 (2010).
11. H. Kangas *et al.*, Characterization of fibrillated celluloses. A short review and evaluation of characteristics with a combination of methods. *Nordic Pulp & Paper Research Journal* **29**, 129-143 (2014).
12. K. Oksman, A. P. Mathew, M. Sain, Novel bionanocomposites: processing, properties and potential applications. *Plastics, rubber and composites* **38**, 396-405 (2009).
13. C. Moser, M. E. Lindström, G. Henriksson, Toward industrially feasible methods for following the process of manufacturing cellulose nanofibers. *BioResources* **10**, 2360-2375 (2015).
14. Y. Qing *et al.*, A comparative study of cellulose nanofibrils disintegrated via multiple processing approaches. *Carbohydrate polymers* **97**, 226-234 (2013).
15. S. Ahola, M. Österberg, J. Laine, Cellulose nanofibrils—adsorption with poly (amideamine) epichlorohydrin studied by QCM-D and application as a paper strength additive. *Cellulose* **15**, 303-314 (2008).
16. K. Benhamou, A. Dufresne, A. Magnin, G. Mortha, H. Kaddami, Control of size and viscoelastic properties of nanofibrillated cellulose from palm tree by varying the TEMPO-mediated oxidation time. *Carbohydrate Polymers* **99**, 74-83 (2014).
17. I. Besbes, M. R. Vilar, S. Boufi, Nanofibrillated cellulose from alfa, eucalyptus and pine fibres: preparation, characteristics and reinforcing potential. *Carbohydrate Polymers* **86**, 1198-1206 (2011).
18. A. Chaker, S. Alila, P. Mutjé, M. R. Vilar, S. Boufi, Key role of the hemicellulose content and the cell morphology on the nanofibrillation effectiveness of cellulose pulps. *Cellulose* **20**, 2863-2875 (2013).
19. A. Naderi, T. Lindström, J. Sundström, Repeated homogenization, a route for decreasing the energy consumption in the manufacturing process of carboxymethylated nanofibrillated cellulose? *Cellulose* **22**, 1147-1157 (2015).
20. O. Nechyporchuk, M. N. Belgacem, J. Bras, Production of cellulose nanofibrils: A review of recent advances. *Industrial Crops and Products* **93**, 2-25 (2016).

21. T. Saito, Y. Nishiyama, J.-L. Putaux, M. Vignon, A. Isogai, Homogeneous suspensions of individualized microfibrils from TEMPO-catalyzed oxidation of native cellulose. *Biomacromolecules* **7**, 1687-1691 (2006).
22. S. Iwamoto, K. Abe, H. Yano, The effect of hemicelluloses on wood pulp nanofibrillation and nanofiber network characteristics. *Biomacromolecules* **9**, 1022-1026 (2008).
23. G. Chinga-Carrasco, Optical methods for the quantification of the fibrillation degree of bleached MFC materials. *Micron* **48**, 42-48 (2013).
24. A. Tanaka, V. Seppänen, J. Houni, A. Sneek, P. Pirkonen, BIOREFINERY. Nanocellulose characterization with mechanical fractionation. *Nordic Pulp & Paper Research Journal* **27**, 689-694 (2012).
25. K. Syverud, G. Chinga-Carrasco, J. Toledo, P. G. Toledo, A comparative study of Eucalyptus and Pinus radiata pulp fibres as raw materials for production of cellulose nanofibrils. *Carbohydrate Polymers* **84**, 1033-1038 (2011).
26. J. Desmaisons, E. Boutonnet, M. Rueff, A. Dufresne, J. Bras, A new quality index for benchmarking of different cellulose nanofibrils. *Carbohydrate Polymers* **174**, 318-329 (2017).
27. R. E. Abouzeid, R. Khiari, N. El-Wakil, A. J. B. Dufresne, Current state and new trends in the use of cellulose nanomaterials for wastewater treatment. **20**, 573-597 (2018).
28. M. L. Hassan *et al.*, Water purification ultrafiltration membranes using nanofibers from unbleached and bleached rice straw. *Scientific Reports* **10**, 11278 (2020).
29. M. L. H. Mohamed Taha, Montasser Dewidare, M.A. kamel, W. Y. Ali, Alain Dufresne, TRIBOLOGICAL BEHAVIOR OF ULTRA-HIGH MOLECULAR WEIGHT POLYETHYLENE NANOCOMPOSITES %J Journal of the Egyptian Society of Tribology. **18**, 27-41 (2021).
30. R. E. Abouzeid, R. Khiari, D. Beneventi, A. J. B. Dufresne, Biomimetic mineralization of three-dimensional printed alginate/TEMPO-oxidized cellulose nanofibril scaffolds for bone tissue engineering. **19**, 4442-4452 (2018).
31. R. E. Abouzeid *et al.*, In situ mineralization of nano-hydroxyapatite on bifunctional cellulose nanofiber/polyvinyl alcohol/sodium alginate hydrogel using 3D printing. *International Journal of Biological Macromolecules* **160**, 538-547 (2020).
32. A. Abdal-hay *et al.*, Engineering of electrically-conductive poly(ϵ -caprolactone)/ multi-walled carbon nanotubes composite nanofibers for tissue engineering applications. *Ceramics International* **45**, 15736-15740 (2019).
33. H. M. Mousa, K. H. Hussein, M. M. Sayed, M. K. Abd El-Rahman, H.-M. Woo, Development and Characterization of Cellulose/Iron Acetate Nanofibers for Bone Tissue Engineering Applications. **13**, 1339 (2021).
34. B. L. Browning, Methods of wood chemistry. Volumes I & II. *Methods of wood chemistry. Volumes I & II.*, (1967).
35. L. E. Wise, Chlorite holocellulose, its fractionation and bearing on summative wood analysis and on studies on the hemicelluloses. *Paper Trade* **122**, 35-43 (1946).
36. D. Sidiras, D. Koullas, A. Vgenopoulos, E. Koukios, Cellulose crystallinity as affected by various technical processes. *Cellulose chemistry and technology* **24**, 309-317 (1990).
37. S. Park, J. O. Baker, M. E. Himmel, P. A. Parilla, D. K. Johnson, Cellulose crystallinity index: measurement techniques and their impact on interpreting cellulase performance. *Biotechnology for Biofuels* **3**, 10 (2010).
38. L. Berglund *et al.*, Switchable ionic liquids enable efficient nanofibrillation of wood pulp. *Cellulose* **24**, 3265-3279 (2017).
39. E. A. Hassan, M. L. Hassan, Rice straw nanofibrillated cellulose films with antimicrobial properties via supramolecular route. *Industrial Crops and Products* **93**, 142-151 (2016).
40. M. L. Hassan, A. P. Mathew, E. A. Hassan, N. A. El-Wakil, K. Oksman, Nanofibers from bagasse and rice straw: process optimization and properties. *Wood science and technology* **46**, 193-205 (2012).
41. D. K. Owens, R. C. Wendt, Estimation of the surface free energy of polymers. *Journal of Applied Polymer Science* **13**, 1741-1747 (1969).
42. W. Rabel, Flüssigkeitsgrenzflächen in Theorie und Anwendungstechnik. *Physikalische Blätter* **33**, 151-161 (1977).
43. B. Jańczuk, T. Białopiotrowicz, W. Wójcik, The components of surface tension of liquids and their usefulness in determinations of surface free energy of solids. *Journal of Colloid and Interface Science* **127**, 59-66 (1989).
44. K. Gebhardt, *Grundlagen der physikalischen Chemie von Grenzflächen und Methoden zur Bestimmung grenzflächenenergetischer Probleme.* (IGB, 1982).
45. A. D. French, M. S. J. C. Cintrón, Cellulose polymorphy, crystallite size, and the Segal crystallinity index. **20**, 583-588 (2013).
46. E. C. Lengowski, G. I. B. d. Muñiz, A. S. d. Andrade, L. C. Simon, S. J. R. Á. Nisgoski,

- Caracterização morfológica, física e térmica de celuloses microfibriladas. **42**, (2018).
47. E. Sjöstrom, *Wood chemistry: fundamentals and applications*. (Gulf professional publishing, 1993).
 48. H. Kawamoto, T. Watanabe, S. J. J. o. a. Saka, a. pyrolysis, Strong interactions during lignin pyrolysis in wood—A study by in situ probing of the radical chain reactions using model dimers. **113**, 630-637 (2015).
 49. R. M. Issa, M. M. Abou-Sekkina, A. M. Khedr, A. E.-D. M. Bastawisy, W. A. J. A. J. o. C. El-Helece, Trace the exploitation of Egyptian rice straw through spectral and thermal measurements. **9**, S130-S137 (2016).
 50. E. Espinosa *et al.*, PVA/(ligno)nanocellulose biocomposite films. Effect of residual lignin content on structural, mechanical, barrier and antioxidant properties. *International Journal of Biological Macromolecules* **141**, 197-206 (2019).
 51. G. Chinga-Carrasco *et al.*, Bleached and unbleached MFC nanobarriers: properties and hydrophobisation with hexamethyldisilazane. *Journal of nanoparticle research* **14**, 1280 (2012).
 52. F. Rol, N. Belgacem, V. Meyer, M. Petit-Conil, J. Bras, Production of fire-retardant phosphorylated cellulose fibrils by twin-screw extrusion with low energy consumption. *Cellulose* **26**, 5635-5651 (2019).
 53. F. Rol, B. Vergnes, N. El Kissi, J. Bras, Nanocellulose production by twin-screw extrusion: simulation of the screw profile to increase the productivity. *ACS Sustainable Chemistry & Engineering* **8**, 50-59 (2019).
 54. E. J. Foster *et al.*, Current characterization methods for cellulose nanomaterials. *Chemical Society Reviews* **47**, 2609-2679 (2018).
 55. E. Espinosa, F. Rol, J. Bras, A. Rodríguez, Use of multi-factorial analysis to determine the quality of cellulose nanofibers: effect of nanofibrillation treatment and residual lignin content. *Cellulose*, 1-17 (2020).
 56. F. Rol, G. Banvillet, V. Meyer, M. Petit-Conil, J. Bras, Combination of twin-screw extruder and homogenizer to produce high-quality nanofibrillated cellulose with low energy consumption. *Journal of Materials Science* **53**, 12604-12615 (2018).